

Journal of Materials Chemistry B

Accepted Manuscript



This is an *Accepted Manuscript*, which has been through the Royal Society of Chemistry peer review process and has been accepted for publication.

Accepted Manuscripts are published online shortly after acceptance, before technical editing, formatting and proof reading. Using this free service, authors can make their results available to the community, in citable form, before we publish the edited article. We will replace this *Accepted Manuscript* with the edited and formatted *Advance Article* as soon as it is available.

You can find more information about *Accepted Manuscripts* in the [Information for Authors](#).

Please note that technical editing may introduce minor changes to the text and/or graphics, which may alter content. The journal's standard [Terms & Conditions](#) and the [Ethical guidelines](#) still apply. In no event shall the Royal Society of Chemistry be held responsible for any errors or omissions in this *Accepted Manuscript* or any consequences arising from the use of any information it contains.

Conjugating Curcumin to Water Soluble Polymer Stabilized Gold Nanoparticles *via* pH Responsive Succinate Linker

Soma Dey and K. Sreenivasan*

Laboratory for Polymer Analysis, Biomedical Technology Wing, Sree Chitra Tirunal Institute for Medical Sciences and Technology, Poojappura, Trivandrum 695012, India

* Corresponding Author. Telephone: +91-471-2520248; Fax: +91-471-2341814; E-mail: sreeni@sctimst.ac.in

ABSTRACT

Curcumin is a natural product with immense medicinal assets. The low aqueous solubility and consequent poor bioavailability of curcumin are the serious limitations to its utilization as a potential therapeutic agent. In order to enhance the aqueous solubility and bioavailability of the drug, we covalently conjugated curcumin onto the surface of Gold Nanoparticles (AuNPs) aided by a water soluble polymer *via* succinate linker. Conjugation of curcumin was confirmed by Fluorescence, FTIR, ¹H NMR and UV-Visible spectroscopy and XRD studies. The size and surface charge of the AuNPs were determined by DLS and the morphology was visualized by TEM. Aqueous solubility of curcumin was augmented upon conjugation with the polymer stabilized AuNPs. pH responsive release of curcumin from the nano-vehicle ensures safer delivery of the drug at physiological pH. Cytotoxic potential and cellular uptake of curcumin conjugated AuNPs were assessed by MTT assay and fluorescence microscopy respectively using C6 glioma cancer cells. Thus, the curcumin conjugated polymer stabilized AuNPs circumvent limitations of curcumin and can find applications in pH responsive drug delivery.

Introduction

Curcumin is a natural polyphenolic compound extracted from the rhizome of the plant *Curcuma longa* (turmeric). Curcumin is well known as a potent chemotherapeutic and chemopreventive agent with low intrinsic toxicity.¹ Within the last couple of decades, extensive research work has revealed a variety of pharmacological activities in curcumin such as antioxidant, anti-inflammatory, antiproliferative and antiangiogenic activities.²⁻⁶ It has also been reported that the –OH and –OMe groups in curcumin are responsible for its antioxidant and antiproliferative properties respectively.⁷ Curcumin inhibits several important cellular targets such as nuclear transcription factor NF- κ B resulting in blockage of the function of protein Kinase C, Her-2 and epidermal growth factor and thus induces apoptosis. Development of resistance to curcumin is less likely as it can induce apoptosis *via* multiple cell signaling pathways.^{7, 8} However, the main demerit associated with curcumin is its poor bioavailability originating from its hydrophobic nature, rapid metabolism and its physicochemical and biological instability.⁹ In order to redress these problems, several approaches have been proposed. Among them conjugation of curcumin to several water soluble polymers like polyethylene glycol, hyaluronic acid, sodium alginate *etc.*; encapsulation of curcumin in the hydrophobic core of diverse micelles and liposomes *etc.* are worthy to be mentioned.¹⁰⁻¹⁴

Nanotherapeutics can surmount several limitations of conventional drug delivery systems such as low therapeutic indices, lack of water solubility, non-specific biodistribution *etc.*^{15, 16} Over the past decades several nanocarriers have been utilized for safer drug delivery with increased therapeutic efficacy. Among them Gold Nanoparticles (AuNPs) have been extensively used as the vector for various types of drug molecules including anticancer therapeutics.¹⁷⁻¹⁹ AuNPs have

emerged as the potential drug delivery vehicle because of its striking features^{20, 21} like low cytotoxicity, non-immunogenicity, excellent stability in the nanoscale, easy synthesis and functionalization along with tunable surface properties *etc.* Another important aspect is that, suitably functionalized AuNPs usually have much smaller sizes desired for passive targeting to tumor tissues *via* the enhanced permeation and retention (EPR) effect and they have reduced clearance through reticuloendothelial system (RES).^{22, 23}

Herein we report the development of a delivery vehicle for curcumin based on water soluble polymer stabilized AuNPs for the enhancement of aqueous solubility and bioavailability of the hydrophobic drug. To fabricate the nanocarrier, AuNPs were first stabilized with a water soluble, low molecular weight polymer (P1) to give P1 stabilized AuNPs (P1-AuNPs) which was subsequently modified via succinylation producing P1-AuNPs with succinate linker (SA-P1-AuNPs). Finally curcumin conjugated AuNPs (Ccm-SA-P1-AuNPs) were developed by conjugation of curcumin to the succinate linker through esterification reaction. The physicochemical properties of Ccm-SA-P1-AuNPs were characterized and *in vitro* cytotoxicity assessment was carried out against Glial cells from rat glioma (C6 Glioma) to prove the retention of intrinsic antiproliferative activity of curcumin after covalent conjugation onto the surface of polymer functionalized AuNPs. Cellular uptake of FITC tagged Ccm-SA-P1-AuNPs was visualized by fluorescence microscope. The curcumin conjugated AuNPs also clearly exhibited the characteristic surface plasmon resonance band signifying its potential applications for imaging that can also be explored.²⁴

Experimental

Materials

Hydrogentetrachloroaurate(III)trihydrate ($\text{HAuCl}_4 \cdot 3\text{H}_2\text{O}$), sodium citrate tribasic dihydrate, citric acid (CA), Polyethylene glycol of average molecular weight 200 (PEG), L-Cysteine (L-Cys), Succinicanhydride (SA), 4-Dimethylaminopyridine (DMAP), 1,3-Dicyclohexylcarbodiimide (DCC) and Triethylamine (TEA) were purchased from Sigma-Aldrich (Bangalore, India). Curcumin (Ccm), from turmeric rhizome and 95% total curcuminoid content, was obtained from Alfa Aesar (Chennai, India). Dimethyl sulfoxide (DMSO) and ethanol (EtOH) were obtained from Merck (Mumbai, India). Hydrochloric acid (HCl) and sodium hydroxide (NaOH) were purchased from Merck (Mumbai, India). In all the experiments ultrapure water (18.2 m Ω resistivity, obtained from Milli-Q water purification system) was used.

Glioma cells were obtained from the National Centre for Cell Sciences (NCCS), Pune, India. 3-(4,5-Dimethylthiazol-2-yl)-2,5-diphenyl tetrazolium bromide (MTT reagent), fetal bovine serum (FBS) and Dulbecco's Modified Eagle's Medium were purchased from Sigma-Aldrich (Bangalore, India). Trypsin/EDTA and Nutrient F-12 Ham were purchased from Invitrogen (Bangalore, India).

Synthesis of low molecular weight polymer P1 and P1 stabilized AuNPs

The water soluble, low molecular weight polymer P1 was synthesized as reported elsewhere with a little modification.²⁵ In brief, equimolar amounts of CA and PEG were taken in a three necked round bottom flask fitted with a mechanical stirrer. Reactants were melted at 160 °C temperature with gradual addition of L-Cys (molar ratio of L-Cys: CA 0.2) under inert atmosphere. Reaction mixture was allowed to react at 160 °C for about 15 minutes and then the temperature was kept at 140 °C for about one hour with constant stirring. The highly viscous polymer P1 was transferred to a separate beaker in hot condition and then cooled to room temperature. P1 was

purified by dialysis against water and lyophilized. P1 was stored in refrigerator in an amber colored glass bottle for further studies.

P1-AuNPs were generated from citrate-AuNPs via ligand exchange reaction. Citrate-AuNPs were prepared by Turkevich method.²⁶ Briefly, to a boiling solution of $\text{HAuCl}_4 \cdot 3\text{H}_2\text{O}$ (20 mL, 1.0 mM), 1% (w/v) aqueous solution of sodium citrate tribasic dihydrate (2 mL) was added under constant stirring. The solution showed a color change from pale yellow through bluish-black to wine red. The wine red solution was cooled and mixed with aqueous solution of P1 (1 mg/mL). The solution mixture was kept under moderate stirring at 25 °C for about 10 hours. Finally the solution was centrifuged for 20 min at 10,000 revolutions per minute (rpm) with an ultracentrifuge (Sigma 3-30 K, Germany) and washed with water to get the P1- AuNPs. The P1-AuNPs were used for further studies.

Covalent conjugation of curcumin to P1-AuNPs

Curcumin was conjugated to P1-AuNPs through a succinate linker following a two step synthetic approach. In the first step, the capping polymer P1 bearing free –OH groups was succinylated using excess SA.²⁷ To a dispersion of P1-AuNPs in $\text{H}_2\text{O}/\text{DMSO}$ (3:1 v/v) mixture containing catalytic amount of DMAP, SA was added in small portions. The solution was stirred well and pH was maintained at 9 by dropwise addition of TEA. The reaction mixture was stirred for 16 hrs at 25 °C. Then it was centrifuged (10000 rpm, 20 min) and thoroughly washed with water to get SA-P1-AuNPs.

In the second step, curcumin was conjugated to the succinate linker available in SA-P1-AuNPs. Aqueous suspension of SA-P1-AuNPs (10 mg in 10 mL) was stirred with 200 μL DCC (4 mM, in DMSO) and 150 μL DMAP (4 mM, in DMSO) for 2 hrs at room temperature to activate the –

COOH groups on NPs' surface. After that 150 μL curcumin solution (4 mM, in DMSO) was added to it and the reaction mixture was stirred overnight at 25 $^{\circ}\text{C}$. The solution was then centrifuged (10000 rpm, 15 min) and washed properly (with both water/DMSO mixture and water) to remove the vestigial molecules. Finally the curcumin conjugated AuNPs (Ccm-SA-P1-AuNPs) were dispersed in ultrapure water (10 mL) and this solution was used for further studies.

Physicochemical characterization

To obtain the Fourier Transform Infrared (FTIR) spectra in the range of 4000-400 cm^{-1} , a Nicolet model 5700 FTIR spectrometer (Nicolet Inc., Madison, USA) was used. Nuclear Magnetic Resonance (^1H NMR) spectra was analyzed by 500 MHz spectrometer (Bruker Avance DPX 500). NMR spectra of P1 and Ccm-SA-P1-AuNPs were recorded in DMSO- D_6 and D_2O with a drop of DMSO- D_6 solvents respectively, at room temperature. Formation of citrate-AuNPs and its surface modifications thereafter were analyzed by recording the surface plasmon resonance (SPR) absorption of the AuNPs by Ultraviolet-Visible (UV-Vis) spectroscopy (Varian model Cary Win Bio 100 spectrophotometer, Melbourne, Australia) using quartz cuvettes of 1 cm path length. The hydrodynamic diameter and zeta potential were measured using a dynamic light scattering (DLS) instrument (Malvern Zetasizer Nano ZS, Malvern Instruments Ltd., Malvern, UK) with a He-Ne laser beam at a wavelength of 633.8 nm. The morphology of the developed AuNPs were viewed by Transmission Electron microscope (TEM; HITACHI, H-7650, Tokyo, Japan). Samples for TEM analysis were prepared by depositing 10 μL of aqueous suspension of AuNPs on a 200 mesh copper grid with formvar film and air drying it at room temperature. Fluorescence spectra of P1 and P1-AuNPs were recorded using a spectrofluorometer (Cary Eclipse model EL 0507). Gel Permeation Chromatography (GPC) (Waters Assoc Inc.; Mailford,

USA, model 600 pumps) was performed to determine number and weight average molecular weight of P1. Waters Styragel column (HR5E/4E/2/0.5 columns in series) and THF were used as the stationary phase and mobile phase respectively. Polystyrene molecular weights standards were used for column calibration. The powder X-ray diffraction (XRD) patterns of pure curcumin and curcumin conjugated P1-AuNPs were recorded with X-ray diffractometer (Bruker D8 Advance; equipped with Cu K α radiation source) from 10° to 90° (2 θ angle).

Determination of stability of Ccm-SA-P1-AuNPs

The stability of Ccm-SA-P1-AuNPs in different concentration of NaCl solutions (0.01-1M) and at different pH values (1.5-12) were measured by UV-Vis absorption spectroscopy. The pH of the aqueous dispersion of Ccm-SA-P1-AuNPs was adjusted by addition of 0.1 M HCl or 0.1 M NaOH solution.

Determination of curcumin content in Ccm-SA-P1-AuNPs

After synthesis and purification of Ccm-SA-P1-AuNPs by centrifugation, the NPs' pellets were fridge dried. A known amount of the dry sample was then added to a known volume of EtOH and the mixture was kept in an orbital shaker for 24 h (at 37 °C and at 120 rpm). Then it was centrifuged (14,000 rpm, 15 min) and the supernatant was carefully collected. The collected solution was diluted with distilled water and curcumin present in the solution was quantified from a calibration plot ($R^2 = 0.997$) using UV-Vis spectrophotometer (at $\lambda_{\text{max}} = 427$ nm).

Study of curcumin release from Ccm-SA-P1-AuNPs

The release of Ccm from Ccm-SA-P1-AuNPs was determined by dialysis bag method at different pHs (phosphate buffer of pH 7.4 and 5.3) at 37 °C. Prior to the study, the dialysis

membrane (MWCO 500) was soaked in water for 1h. Then Ccm-SA-P1-AuNPs was placed in the dialysis bag with two end fixed by clamps and the dialysis bag was suspended in 10 mL of release medium (Phosphate buffer of pH = 5.3). The bag was incubated at 37 °C, 120 rpm in a glass vessel. Release medium was removed periodically and an equal volume of fresh buffer solution (pH = 5.3) was added to the glass vessel. The sample removed was diluted with ethanol and analyzed using UV-Vis absorption spectroscopic technique. Similar experiment was carried out with phosphate buffer (pH = 7.4) to evaluate the release profile of the nano-carrier under physiological condition.

Cytotoxicity evaluation of Ccm-SA-P1-AuNPs

The cytotoxic potential of Ccm-SA-P1-AuNPs was quantified by MTT assay against Glial cells from rat glioma (C6 Glioma). In brief, C6 cells were maintained in 50:50 mixture of Dulbecco's Modified Eagle's Medium/Nutrient F-12 Ham and MEM supplemented with 10% FBS. Then 80% confluent cells were trypsinized and seeded in 48 well plates (5×10^4 cells) and incubated for 24 h. Then the cells were exposed to fresh medium containing different concentrations of Ccm-SA-P1-AuNPs and free curcumin in a CO₂ (5%) incubator at 37 °C. After 24 h incubation, the medium containing sample and free drug was removed from respective wells and 200 µL of freshly prepared MTT solution (0.5 mg/mL) in culture medium was added into each well. After 4 h incubation, MTT solution was carefully removed. DMSO (200 µL) was then added into each well and the plate was gently shaken for 10 min at room temperature to dissolve all precipitates formed. The absorbance of individual wells at 570 nm was then detected by a microplate reader (Tecan Infinite M200, Switzerland). Cell viability was expressed as the mean percentage of

sample absorbance relative to untreated cells. Here each reported value is the mean of three replicates.

Cell viability (%) = $\frac{A_s}{A_c} \times 100$, where A_s is the absorbance of sample and A_c is the absorbance of control.

Cellular uptake study using FITC tagged Ccm-SA-P1-AuNPs

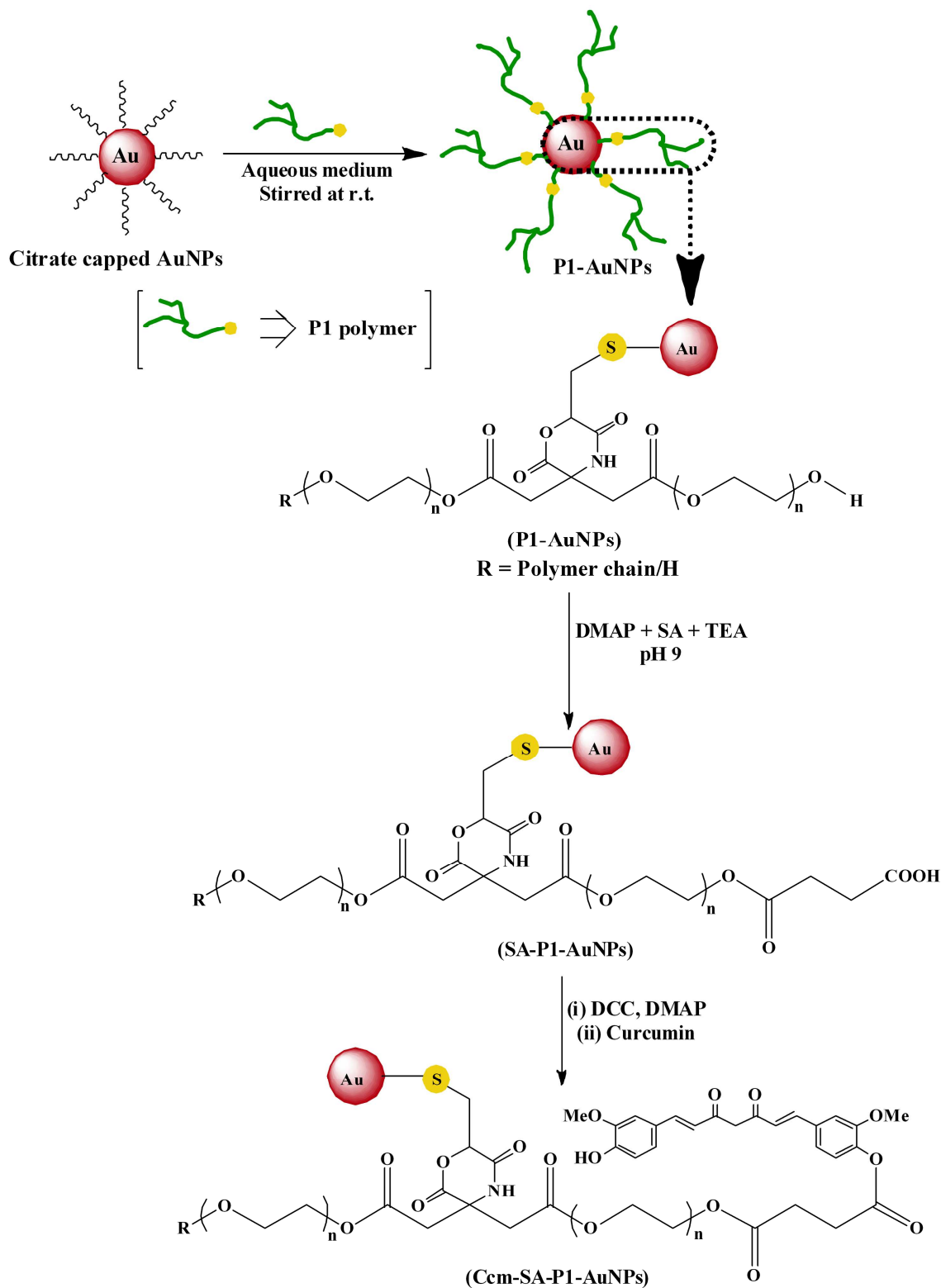
Cellular images were acquired with a fluorescence microscope (Leica DM IRB, Germany) using C6 cell line. Cells were seeded on a 4-well plate at 37 °C for 24 h. After incubating the cells with FITC tagged Ccm-SA-P1-AuNPs for 3 h, the medium containing the nanoparticles was removed from each well and the cells were washed with PBS (twice) to remove any non-specific binding. After fixing the cell, uptake was detected in fluorescence microscope exploiting the fluorescence emission of FITC.

Results and discussion

Herein we report the stabilization of AuNPs by a low molecular weight water soluble polymer P1 and thereafter using P1-AuNPs as a carrier for curcumin with enhanced aqueous solubility and improved bioavailability of the hydrophobic drug. In this study, water soluble polymer P1 was synthesized as reported elsewhere with minor modification.²⁵ The synthetic scheme for P1 is depicted Fig. S1 (Supplementary Information). P1 was characterized using a variety of techniques. The number and weight average molecular weights and the polydispersity index (PDI) of P1 were determined by GPC. The data obtained from GPC are tabulated in Table S1 (Supplementary Information). FTIR spectrum of P1 confirmed the presence of characteristic functionality like -C=O (1727 cm^{-1}), -C(=O)NH- (1520 cm^{-1}) and -S-H (2515 cm^{-1}) in the

polymer chain (Fig. 1A). P1 was found to be photoluminescent in nature. Unlike fluorescent polymers, P1 is devoid of any conjugated phenyl chromophores. P1 bears a ring structure resembling *morpholine-2,5-dione* in its polymer chain (Fig. S1, Supplementary Information). An extensive hyperconjugation present in the heterocyclic ring containing both amide and ester linkages and a pendant $-\text{CH}_2\text{SH}$ group in close vicinity makes P1 fluorescent.²⁵ The characteristic UV-VIS absorption spectra and fluorescence spectra of P1 (aqueous solution, 0.5 % w/v) are shown in Supplementary Information (Fig. S2A, S2B respectively).

The AuNPs based curcumin delivery system (Ccm-SA-P1-AuNPs) was synthesized following a stepwise synthetic route as shown in Scheme 1. In the first step, citrate-AuNPs were prepared by Turkevich method²⁶ and the citrate-AuNPs were modified with P1 following ligand exchange route. P1 bearing free thiol linkage can strongly bind to the surface of AuNPs via Au-S bond and hence imparts excellent stability to the AuNPs. In the second stage of synthesis, P1-AuNPs was succinylated in aqueous alkaline medium (pH = 9) using excess amount of succinic anhydride. The succinylated product (SA-P1-AuNPs) contained free carboxyl groups which were then activated using DCC. The activated $-\text{COOH}$ groups in the succinate linker reacted with phenolic $-\text{OH}$ group of curcumin in presence of catalytic amount of DMAP in $\text{H}_2\text{O}/\text{DMSO}$ mixture resulting in Ccm-SA-P1-AuNPs.



Scheme 1. Schematic presentation of the synthesis of Ccm-SA-P1-AuNPs.

Surface modification of AuNPs at each step of synthesis was confirmed by FTIR analysis as shown in Fig. 1. Fig. 1A and 1B show the FTIR spectrum of pure P1 and P1-AuNPs respectively. The low intensity sharp peak of -SH functionality (at around 2515 cm^{-1}) seen in Fig. 1A was found to be missing in Fig. 1B indicating chemical adsorption of P1 onto the surface of AuNPs via Au-S covalent bond. Besides, Fig. 1B displays peaks corresponding to -C=O stretching frequency at 1711 cm^{-1} , -C-H stretching frequency at 2924 cm^{-1} and 2854 cm^{-1} , free -O-H stretching frequency at 3647 cm^{-1} and -N-H bending vibration at 1462 cm^{-1} . In Fig. 1C a broad band at about 3411 cm^{-1} is assigned to the -O-H stretching frequency and the peak at around 1603 cm^{-1} characteristic to the -C-O stretching of carboxylate anion confirms the succinylation reaction. This peak around 1603 cm^{-1} vanishes as shown in Fig. 1D after Ccm conjugation pointing out that -COO^- is the reaction site. In addition to this, in Fig. 1D a relatively sharp peak at 3420 cm^{-1} associated with the phenolic -OH of Ccm can be seen. The peaks at around 1703 cm^{-1} and 1670 cm^{-1} are assigned to the ester C=O stretching frequency and ketonic functionality in Ccm respectively. A peak at 1290 cm^{-1} attributed to the -C-O stretching frequency of ester reflects conjugation of Ccm onto AuNPs via esterification reaction. Here it is worthy to be mentioned that the characteristic strong fluorescence emission of P1 was quenched as the AuNPs were functionalized with P1 (Fig. S3, Supplementary Information). Quenching of fluorescence of P1 strongly indicates the adsorption of P1 on the surface of AuNPs. This type of quenching effect is observed frequently when a fluorescent species is in close contact with AuNPs.²⁸

As SPR absorption is highly sensitive to the surface environment of NPs²⁹ changes in the SPR absorption were monitored during each step of synthesis of Ccm-SA-P1-AuNPs. Citrate-AuNPs showed a characteristic SPR at 521 nm which was red-shifted to 524 nm in P1-AuNPs indicating chemisorption of P1 onto the surface of AuNPs (as shown in Fig. 2A). Fig. 2B shows further red-

shift of SPR absorption of P1- AuNPs upon succinylation and Ccm conjugation (λ_{\max} at around 527 nm and 531 nm respectively). These shifts in SPR band confirm the surface modification of AuNPs. It is to be noted that the distinct and characteristic absorption peak of curcumin at around 420 nm was not seen in the spectrum as it overlaps with the intense SPR absorption of AuNPs (Fig. 2B). However, another absorption peak of curcumin at around 280 nm was clearly seen (Fig. 2B). Comparison of the SPR absorption spectra of SA-P1-AuNPs and Ccm-SA-P1-AuNPs shown in Fig. 2B (in the range of 200 nm to 800 nm) strongly support the conjugation of curcumin onto the surface of P1-AuNPs. Besides, no significant broadening of the SPR absorption peak was noticed (Fig. 2A and 2B) which indicated that modification steps didn't induced any aggregation among the AuNPs. This observation was supported by the TEM images shown in Fig. 4.

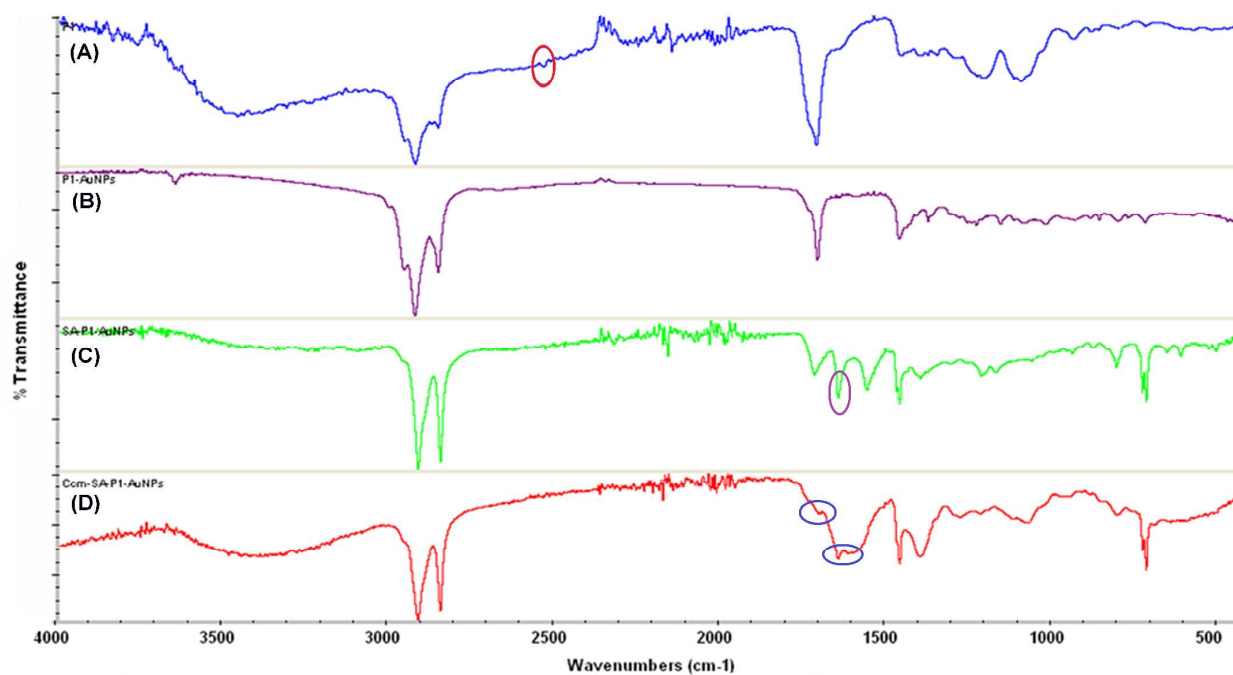


Fig. 1. FTIR spectra of (A) P1; (B) P1-AuNPs; (C) SA-P1-AuNPs and (D) Ccm-SA-P1-AuNPs.

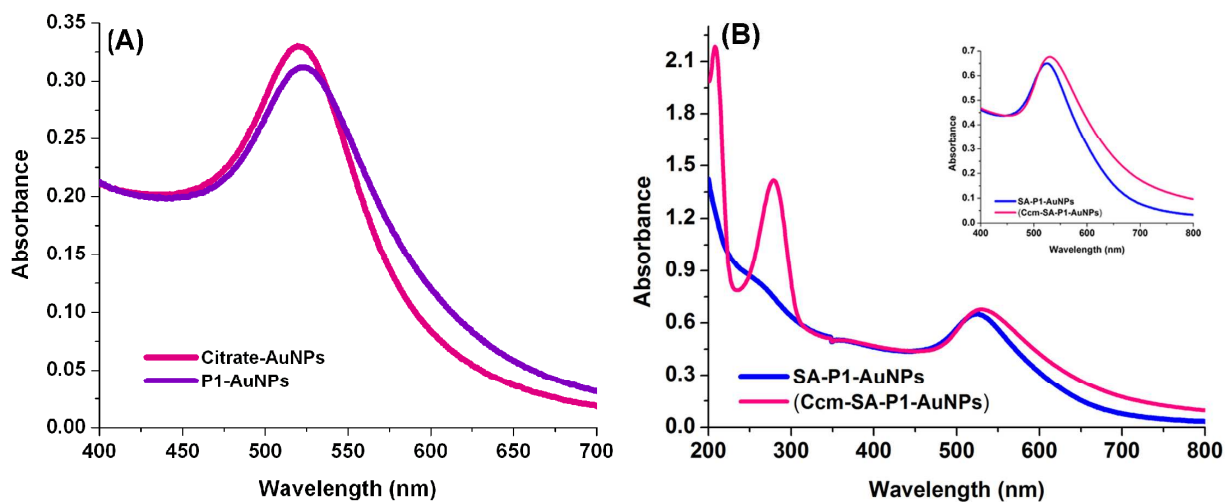


Fig. 2. Surface Plasmon resonance absorption of AuNPs at various stages of modifications (A) red shift in absorbance for P1-AuNPs synthesis from citrate-AuNPs and (B) further red shift in absorbance in formation of SA-P1-AuNPs and Ccm-SA-P1-AuNPs (*inset* absorption spectra of SA-P1-AuNPs and Ccm-SA-P1-AuNPs in the visible range).

The formation of Ccm-SA-P1-AuNPs was further confirmed by ^1H NMR spectra as shown in Fig. 3. In ^1H NMR spectrum of pure P1 (Fig. 3A), the peaks at $\delta \approx 2.7$ ppm can be assigned to the $-\text{CH}_2$ protons of citric acid. Peaks at $\delta \approx 4.3$ ppm are due to the $-\text{CH}_2-\text{CH}_2-\text{O}$ protons from PEG. The characteristic peak at $\delta = 1.3$ ppm (triplet as shown in the expansion in the inset of Fig. 3A, due to $-\text{SH}$ proton) confirms the presence of thiol functionality in P1. Presence of multiple peaks at around 3 ppm can be attributed to the $-\text{CH}_2-\text{SH}$ protons in P1. In the ^1H NMR spectrum of Ccm-SA-P1-AuNPs (in Fig. 3B), new peaks can be seen between $\delta = 6.5$ to 7.9 ppm (due to the aromatic protons in Ccm) and at $\delta = 3.8$ ppm (due to the characteristic $-\text{OCH}_3$ protons in Ccm) confirming curcumin conjugation to polymer stabilized AuNPs.

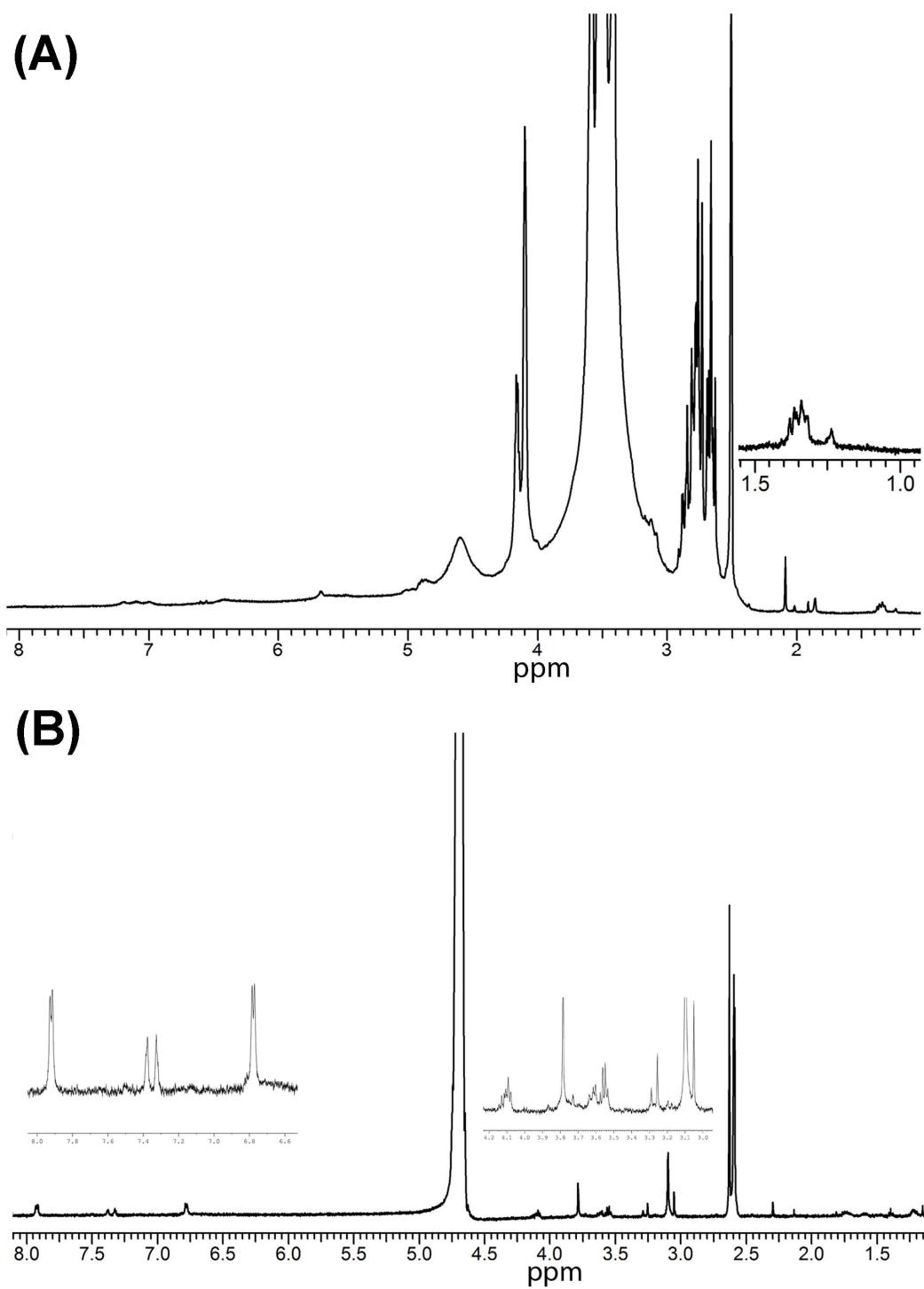


Fig. 3. ^1H NMR spectra of (A) P1 polymer and (B) Ccm-SA-P1-AuNPs.

The hydrodynamic diameter and zeta potential (ζ) of the AuNPs in various steps of modification were measured by DLS at pH 7.4 (in aqueous buffer at 25 °C). The DLS data for the functionalized AuNPs are tabulated in Table 1. The small size of the curcumin conjugated AuNPs might be advantageous to exhibit better EPR effect. The magnitude of ζ -potential of Citrate-AuNPs dropped from -40.2 ± 0.3 mV to -23.1 ± 0.2 mV in P1-AuNPs. This decrease of ζ -potential value may be attributed to PEG (possessing stealth property) which is the backbone for P1³⁰. SA-P1-AuNPs contain free carboxylate groups on its surface and those carboxylates are in deprotonated state ($pK_a = 4.2$)^{31, 32} at pH = 7.4, hence the NPs were found to possess surface charge of -40.9 ± 2.74 mV. After Ccm conjugation the ζ -potential again drops to -32 ± 0.65 mV in Ccm-SA-P1-AuNPs. Though the surface charge was reduced to certain extent after Ccm conjugation, yet there was sufficient repulsive force present in the system to prevent it from aggregation and the TEM image shown in Fig. 4D supports this fact. As the small sized AuNPs are functionalized with a polymer containing PEG as the backbone and they possess negative surface charge, hence the nano drug delivery vehicle may, to a large extent, evade protein adsorption resulting in longer systemic circulation and enhanced EPR effect.^{12, 33}

Table 1. Sizes and zeta potential values of AuNPs solution (25 °C, pH = 7.4) after each step of surface modification.

Material	Hydrodynamic diameter (nm)	Zeta potential (mV)
Citrate -AuNPs	15.60 ± 0.11	-40 ± 0.30
P1-AuNPs	19.7 ± 0.06	-23.1 ± 0.20
SA-P1-AuNPs	25.8 ± 2.30	-40.9 ± 2.74
Ccm-P1-AuNPs	43.10 ± 1.80	-32 ± 0.65

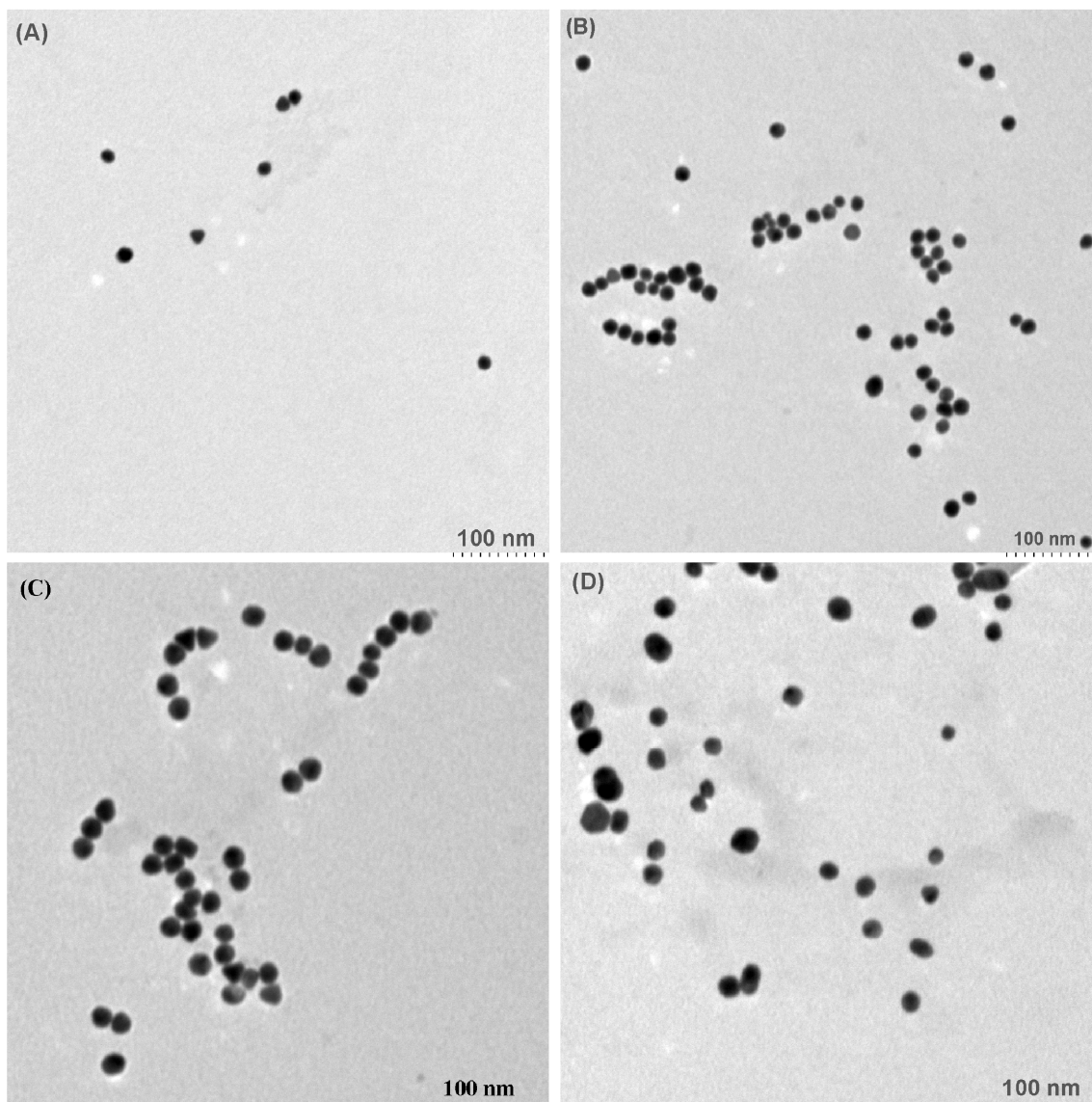


Fig. 4. TEM images of AuNPs at different stages of modification: (A) Citrate AuNPs (B) P1-AuNPs (C) SA-P1-AuNPs and (D) Ccm-SA-P1-AuNPs.

In order to check the stability of the curcumin conjugated P1-AuNPs, the NPs were treated with varying concentrations of NaCl. Ccm-SA-P1-AuNPs were found to withstand high salt

concentration (highly stable in 0.1 M NaCl environment; Fig. 5A). In addition to this, Ccm-SA-P1-AuNPs showed good stability in the physiological pH (pH = 7.4; Fig. 5B). These results indicated that Ccm-SA-P1-AuNPs to be highly stable at physiological condition and the nano system may find potential application as a drug delivery vehicle³⁴.

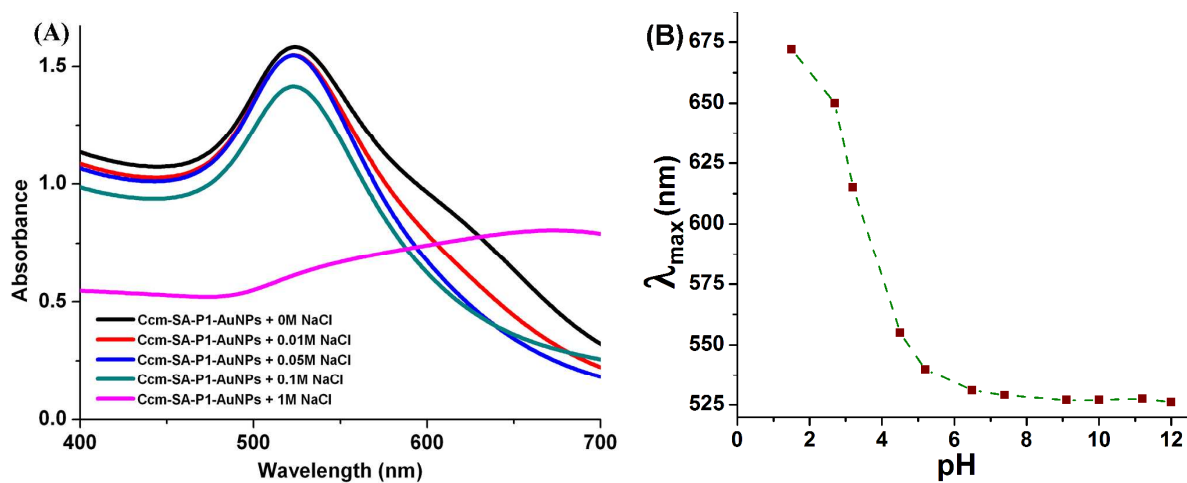


Fig. 5. Determination of the stability of Ccm-SA-P1-AuNPs (A) UV-Vis absorption spectra in different concentrations of NaCl and (B) Change in SPR maxima against pH (1.5 to 12).

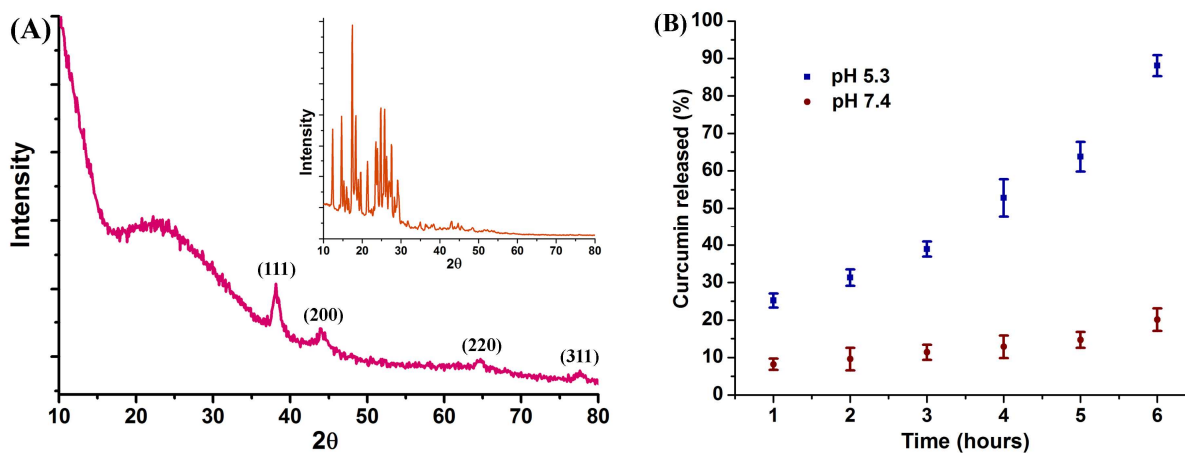


Fig. 6. (A) XRD pattern of Ccm-SA-P1-AuNPs (*inset*: XRD pattern of pure curcumin) and (B) curcumin release profile from Ccm-SA-P1-AuNPs in buffer solution of different pH.

Fig. 6A compares the XRD patterns of pure curcumin and Ccm-SA-P1-AuNPs. The X-ray diffractogram of Ccm-SA-P1-AuNPs clearly depicts the characteristic peaks of face centred cubic (FCC) crystal lattice of drug conjugated polymer stabilized AuNPs.³⁵ In the XRD pattern of curcumin (shown as the *inset* in Fig. 6A) a number of sharp peaks (in the 2θ range of 10° to 30°) indicate the crystalline nature of the hydrophobic drug. However, in Ccm-SA-P1-AuNPs no such crystalline peak of curcumin was observed. This data further confirms that after covalent conjugation onto the surface of AuNPs *via* the water soluble capping polymer, the drug is in amorphous or disordered phase which is highly desired for a regular and unimpeded drug release from the AuNPs.^{12, 36}

The curcumin content in curcumin conjugated P1-AuNPs was determined by UV-Vis spectroscopy. The amount of curcumin extracted from a known amount of Ccm-SA-P1-AuNPs was measured using a calibration plot ($R^2 = 0.997$, $\lambda_{\max} = 427$ nm). The study revealed that 10 mg of Ccm-SA-P1-AuNPs contained 67.5 ± 0.08 μg of curcumin. Curcumin is basically having very poor aqueous solubility. But the curcumin conjugated water soluble polymer capped AuNPs readily get dispersed in water giving rise to a pink suspension. Hence conjugation of curcumin onto the surface AuNPs aided by the water soluble polymer P1 in turn helps in effectively augmenting the solubility of the hydrophobic drug in water.

One of the most important criterion for a drug delivery vehicle is that it should not release the pay load in the blood stream. Covalent conjugation of a drug to the delivery vehicle is far better than the physical adsorption of the drug, provided the covalent bonding is stable enough at the

physiological pH. In this study curcumin was conjugated to the polymer stabilized AuNPs via succinate linker (*i.e.*, through ester linkage). The drug release profile from Ccm-SA-P1-AuNPs shown in Fig. 6B indicates that very low amount of Ccm was released from the nano-carrier at physiological pH over a period of 6 h. Whereas, within the same time span $\approx 90\%$ drug was released at pH 5.3. Thus the release study revealed that Ccm-SA-P1-AuNPs exhibit pH responsive Ccm release behaviour³⁷ and the nano drug delivery vehicle can safely carry the drug through systemic circulation at physiological pH.

Here the AuNPs were stabilized using a water soluble polymer P1 containing free thiol functionality to generate P1-AuNPs. The thiol functional group in P1 originates from the flanking $-\text{CH}_2-\text{(SH)}$ chain of natural amino acid L-Cysteine. The backbone of P1 consists of PEG and CA that are known to be biocompatible. Moreover, in this study curcumin was covalently conjugated to P1-AuNPs via esterification reaction through the succinate linker. One of the phenolic $-\text{OH}$ groups of curcumin reacted with the activated $-\text{COOH}$ functionality on SA-P1-AuNPs to form the ester linkage. It has been mentioned that the therapeutic activity of curcumin may be hindered due to conjugation of the drug through its phenolic $-\text{OH}$ group.²⁴ Herein, the cytotoxic activity of Ccm-SA-P1-AuNPs was evaluated by MTT assay against C6 cancer cells with the aim to check the cytotoxic potential of Ccm conjugated to polymer stabilized AuNPs. MTT assay measures the metabolic reduction of 3-(4,5-dimethylthiazol-2-yl)-2,5-diphenyl tetrazolium bromide to a colored formazan by living cells.

Fig. 7 shows the cytotoxic activity of curcumin conjugated to polymer stabilized AuNPs in comparison with the free drug. Fig. 7 also shows a concentration dependent decrease in cell viability (*i.e.* the more the equivalent concentration of curcumin in the nano-system, the more is

the percentage of cell death and P1-AuNPs was found to be cytocompatible at this concentration as shown in Fig. S4 in Supplementary Information.). The percentage of cell viability quantified by MTT assay indeed proves that the inherent potentiality of the drug to kill cells was not affected by the chemical conjugation. The drug conjugated to P1-AuNPs showed better cytotoxic response compared to that of the free drug. In Ccm-SA-P1-AuNPs, Ccm was covalently conjugated to water soluble polymer P1 and this might have helped the drug to get solubilized in aqueous medium and interact with the cells in a better manner than that of the free drug (Free Ccm may not get better exposure to the cells and may not interact with cells properly due to its poor water solubility and consequent precipitation in aqueous medium). In addition, the improved internalization of small sized Ccm-SA-P1-AuNPs can also be an important attribute to improved cytotoxic response of the drug.

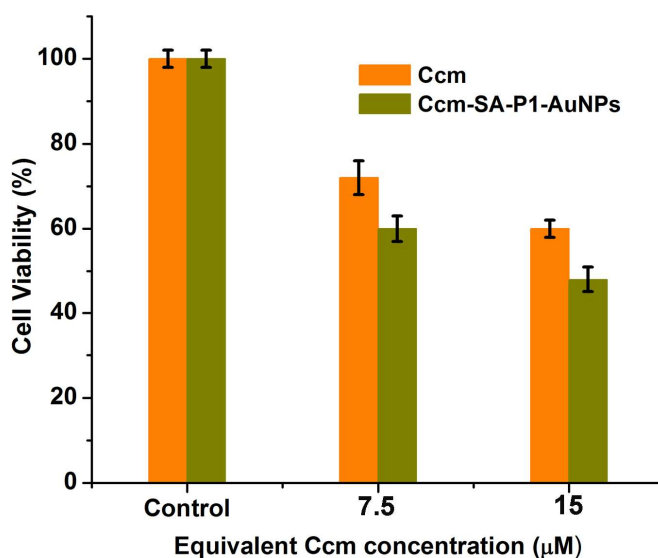


Fig. 7 Cell viability (%) as determined by MTT assay exhibiting the cytotoxicity of Ccm-SA-P1-AuNPs in comparison with free Ccm against C6 cells. The error bars indicate mean \pm standard deviation ($n = 3$).

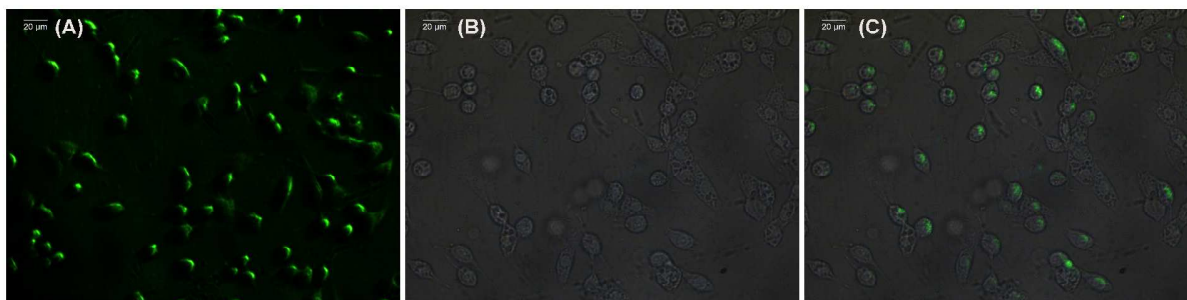


Fig. 8. Fluorescence microscopic images of C6 glioma cells after 3h incubation with FITC tagged Ccm-SA-P1-AuNPs: green fluorescence from FITC (A) fluorescence image (B) bright field image and (C) merged image of green fluorescence in bright field.

In order to confirm the internalization of Ccm-SA-P1-AuNPs, C6 cancer cells were incubated with the FITC tagged Ccm-SA-P1-AuNPs for 3 hours and the uptake of the nanoparticles was visualized by fluorescence microscope exploiting the characteristic green fluorescence of FITC. The fluorescence microscopic images shown in Fig. 8 clearly indicate that the drug conjugated AuNPs were effectively internalized by the cancer cells.

Conclusions

In this study, we reported the direct covalent conjugation of curcumin onto the surface of a water soluble polymer stabilized AuNPs *via* pH responsive succinate linker. The Ccm-SA-P1-AuNPs being small in size can be a very good candidate to exhibit EPR effect. The polymer P1 used to stabilize the AuNPs has PEG as the backbone and hence negatively charged Ccm-SA-P1-AuNPs can avoid protein adsorption to a large extent resulting in enhanced time for systemic circulation and improved EPR effect. Poor water solubility of curcumin is one of the most serious demerits of this polyphenolic drug. This study also reveals that conjugation of curcumin onto the surface of AuNPs using a water soluble polymer eventually augments the aqueous solubility of the hydrophobic drug. Conjugation of curcumin *via* a pH responsive linker assures the safe delivery of the drug through blood stream and at the same time, loss in crystalline nature of curcumin in

Ccm-SA-P1-AuNPs confirms unimpeded release of Ccm from the nano-vehicle. Ccm in Ccm-SA-P1-AuNPs exhibited improved cytotoxic response compared to free drug against C6 cancer cells. Augmented water solubility of Ccm in Ccm-SA-P1-AuNPs and better internalization of the drug conjugated AuNPs can be the two main reasons behind the improved cytotoxicity of the drug in conjugated form. The internalization of the drug conjugated nano-vectors was also confirmed by fluorescence microscopy. In conclusion, conjugation of Ccm to P1-AuNPs *via* succinate linker enhances the aqueous solubility of the hydrophobic drug and cytotoxic Ccm-SA-P1-AuNPs indicates its potential to be utilized in pH responsive drug delivery.

Acknowledgements

The authors gratefully acknowledge the financial assistance provided by CSIR, New Delhi, India to conduct the study. Authors thank and gratefully acknowledge Dr. Rekha M. R. for her kind support in the cellular studies. The authors also thank Director and Head, SCTIMST, Trivandrum for providing the facilities.

References

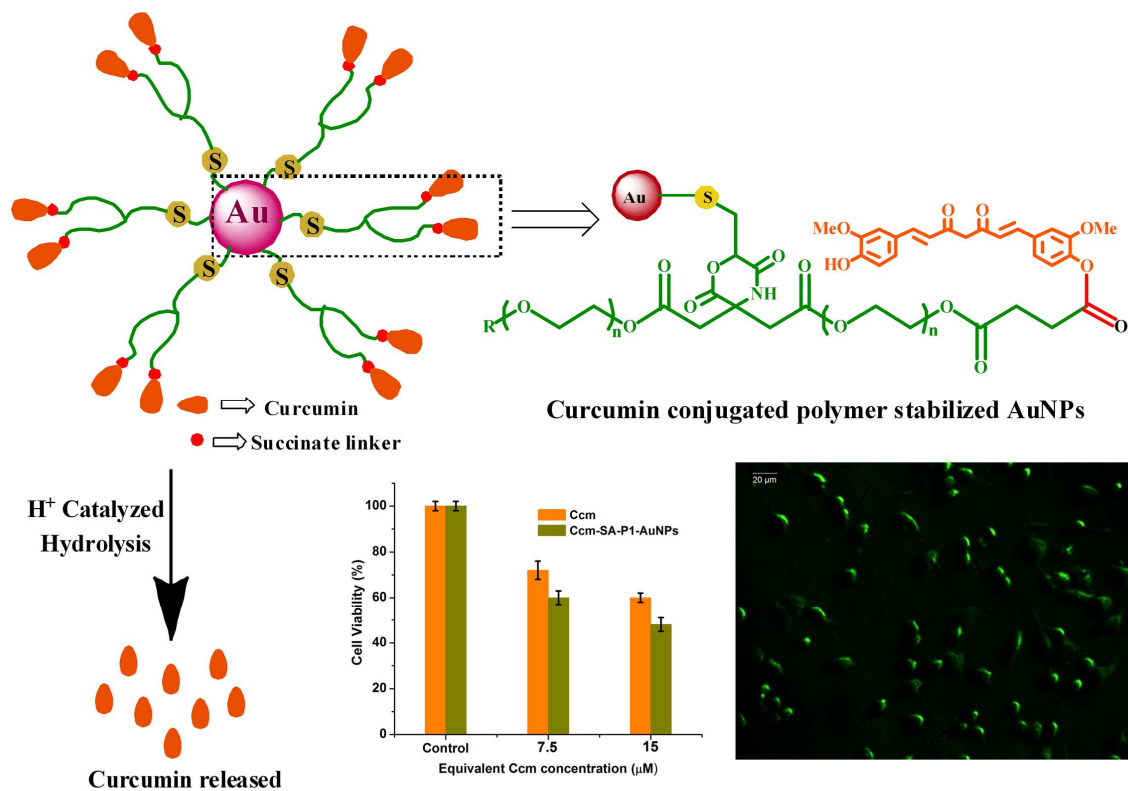
1. A. Duvoix, R. Blasius, S. Delhalle, M. Schnekenburger, F. Morceau, E. Henry, M. Dicato and M. Diederich, *Cancer Letters*, 2005, **223**, 181-190.
2. B. B. Aggarwal, A. Kumar and A. C. Bharti, *Anticancer Res.*, 2003, **23**, 363-398.
3. M. X. Shi, Q. F. Cai, L. M. Yao, Y. B. Mao, Y. L. Ming and G. L. Ouyang, *Cell Biol. Int.* 2006, **30**, 221–226.
4. R. Motterlini, R. Foresti, R. Bassi and C. J. Green, *Free Radical Biol. Med.*, 2000, **28**, 1303- 1312.

5. R. C. Lantz, G. J. Chen, A. M. Solyom, S. D. Jolad and B. N. Timmermann, *Phytomedicine*, 2005, **12**, 445–452.
6. B. B. Aggarwal and B. Sung, *Trends Pharmacol. Sci.* 2009, **30**, 85–94.
7. J. Ravindran, S. Prasad and B. B. Aggarwal, *The AAPS Journal*, 2009, **11**, 495-510.
8. S. Shishodia, H. M. Amin, R. Lai and B. B. Aggarwal, *Biochem. Pharmacol.*, 2005, **70**, 700–713.
9. P. Anand, A. B. Kunnumakkara, R. A. Newman and B. B. Aggarwal, *Mol. Pharmaceutics*, 2007, **4**, 807–818.
10. H. Tang, C. J. Murphy, B. Zhang, Y. Shen, M. Sui, E. A. V. Kirk, X. Feng, and W. J. Murdoch, *Nanomedicine*, 2010, **5**, 855-865.
11. S. Dey and K. Sreenivasan, *Carbohydr. Polym.*, 2014, **99**, 499– 507.
12. A. Anitha, V.G. Deepagan, V. V. D. Rani, D. Menon, S. V. Nair and R. Jayakumar, *Carbohydr. Polym.*, 2011, **84**, 1158–1164.
13. S. Manju and K. Sreenivasan, *J. Colloid Interface Sci.*, 2011, **359**, 318–325.
14. S. Manju and K. Sreenivasan, *J. Pharm. Sci.*, 2011, **100**, 504-511.
15. C. Moorthi, R. Manavalan, K. Kathiresan, *J. Pharm. Pharmaceut. Sci.*, 2011, **14**, 67–77.
16. S. D. Li, L. Huang, *Mol. Pharm.*, 2008, **5**, 496–504.
17. S. Manju and K. Sreenivasan, *J. Colloid Interface Sci.*, 2012, **368**, 144–151.
18. D. R. Bhumkar, H. M. Joshi, M. Sastry and V. B. Pokharkar, *Pharm. Res.*, 2007, **24**, 1415 – 1426.
19. B. Asadishad, M. Vossoughi, and I. Alemzadeh, *Ind. Eng. Chem. Res.*, 2010, **49**, 1958–1963.

20. D. A. Giljohann, D. S. Seferos, W. L. Daniel, M. D. Massich, P.C. Patel, C.A. Mirkin, *Angew. Chem. Int. Ed.*, 2010, **49**, 3280–3294.
21. K. Lee, H. Lee, H. B. Ki and T.G. Park, *Biomaterials*, 2010, **31**, 6530–6536.
22. V. P. Torchilin and V. S. Trubetskoy, *Adv. Drug Delivery Rev.*, 1995, **16**, 141-155.
23. R. Gref, Y. Minamitake, M. T. Peracchia, V. Trubetskoy, V. Torchilin and R. Langer, *Science*, 1994, **263**, 1600-1603.
24. R. K. Gangwar , V. A. Dhumale, D. Kumari, U. T. Nakate, S. W. Gosavi, R. B. Sharma, S. N. Kale, S. Datar, *Mater. Sci. Eng., C*, 2012, **32**, 2659–2663.
25. J. Yang, Y. Zhang, S. Gautam, L. Liu, J. Dey, W. Chen, R. P. Mason, C. A. Serrano, K. A. Schug and L. Tang, *P. Natl. Acad. Sci. USA*, 2009, **106**, 10086-10091.
26. J. Turkevich, P. C. Stevenson and J. Hillier, *Discuss. Faraday Soc.*, 1951, **11**, 55-75.
27. H. Chi, K. Xu, D. Xue, C. Song, W. Zhang and P.Wang, *Food Res. Int.*, 2007, **40**, 232–238.
28. G. Schneider, G. Decher, N. Nerambourg, R. Praho, M. H. V. Werts and M. B. Desce, *Nano Lett.*, 2006, **6**, 530-536.
29. M. Liang, I. C. Lin, M. R. Whittaker, R. F. Minchin, M. J. Monteiro and I. Toth, *ACS Nano*, 2010, **4**, 403-413.
30. J. Manson, D. Kumar, B. J. Meenan and D. Dixon, *Gold bull.*, 2011, **44**, 99-105.
31. S. H. Baek, W. J. Chang, J. Y. Baek, D. S. Yoon, R. Bashir and S. W. Lee, *Anal. Chem.*, 2009, **81**, 7737–7742.
32. A. Biswas, R. L. Shogren, S. Kim and J. L. Willett, *Carbohydr. Polym.*, 2006, **64**, 484–487.

33. S. Aryal, J. J. Grailer, S. Pilla, D. A. Steeberb and S. Gong, *J. Mater. Chem.*, 2009, **19**, 7879–7884.
34. Z. Zhang, J. Jia, Y. Lai, Y. Ma, J. Weng and L. Sun, *Bioorg. Med. Chem.*, 2010, **18**, 5528–5534.
35. K. S. Kim, S. Choi, J. H. Cha, S. H. Yeon and H. Lee, *J. Mater. Chem.*, 2006, **16**, 1315–1317.
36. M. Guo, F. Muhammad, A. Wang, W. Qi, N. Wang, Y. Guo, Y. Weic and Guangshan Zhu, *J. Mater. Chem. B*, 2013, **1**, 5273–5278.
37. C. Clawson, L. Ton, S. Aryal, V. Fu, S. Esener and L. Zhang, *Langmuir*, 2011, **27**, 10556–10561.

Graphical Abstract



Drug amended polymer stabilized gold nanoparticles as pH responsive drug delivery nano vehicles.